JOURNAL OF CATALYSIS **173,** 28–42 (1998)
ARTICLE NO. CA971879

Structure–Activity Relationships in the Ammoxidation of Ethylene in the Absence of Molecular Oxygen over γ-Al_2O_3-Supported Molybdenum Oxide Catalysts

I. Peeters,*,[1] A. W. Denier van der Gon,† M. A. Reijme,† P. J. Kooyman,‡ A. M. de Jong,* J. van Grondelle,* H. H. Brongersma,*,† and R. A. van Santen*

*Schuit Institute of Catalysis, Department of Inorganic Chemistry and Catalysis, †Faculty of Technical Physics, Eindhoven University of Technology, P.O. Box 513, 5600 MB Eindhoven, The Netherlands; and ‡National Center for High Resolution Electron Microscopy, Rotterdamseweg 137, 2628 AL Delft, The Netherlands

Received March 25, 1997; revised August 4, 1997; accepted August 13, 1997

This study focuses on the structure–activity relationships in the reaction of ethylene with ammonia to acetonitrile in the absence of gaseous oxygen over γ-Al_2O_3-supported molybdenum catalysts. Previous work has proved that this reaction is structure-sensitive and that two mechanisms for the formation of acetonitrile exist. The first mechanism is based on ammoxidation with consumption of lattice oxygen and operates on freshly calcined catalysts. The second mechanism operates without the consumption of lattice oxygen on catalysts submitted to long reaction times, independent of pretreatment, and thus, it is based on oxidative ammonolysis. By applying various physico-chemical techniques, such as XRD, HREM, XPS, and LEIS, different solid state properties of the catalyst were identified. Catalysts were analysed right after pretreatment and at different times on stream. From this a relationship was derived between the solid state property of the catalyst and its catalytic property. On freshly calcined catalysts molybdenum is present as $Al_2(MoO_4)_3$ which is highly dispersed on the γ-Al_2O_3 surface. At a loading of 10 wt% Mo, where the maximum adsorption capacity of alumina is exceeded, only 77% of the γ-Al_2O_3 is covered with $Al_2(MoO_4)_3$, indicating that adsorption occurs at specific sites. The ammoxidation mechanism is suggested to be active on this $Al_2(MoO_4)_3$ structure. When the catalyst is pretreated with hydrogen, the molybdenum surface species are best described as MoO_2-like. A decrease in the dispersion of approximately 50% was found upon hydrogen pretreatment. It was also shown that, after long reaction times (>24 h), a highly dispersed MoO_2-like structure was formed, independent of the pretreatment, containing both Mo(IV) and Mo(VI) ions which had reached a structural and chemical equilibrium. It was concluded that the oxidative ammonolysis mechanism is operational on this structure.

INTRODUCTION

Catalysts based upon Mo/Al_2O_3 are remarkable for the variety of reactions they promote. Despite numerous investigations, the basis of their catalytic performance is still unclear. A fundamental understanding of the structure–activity relationships observed in heterogeneous catalytic oxidation is of basic importance for the development of new catalytic materials and for improving the performance of existing catalysts. The activity of these catalysts, determined by their chemical and phase composition, depends on details of preparation and activation.

In catalytic (amm)oxidation, one of the most important questions concerning the reaction mechanism is whether the lattice oxygen participates in the formation of reaction products, implying structure sensitivity. At the surfaces of metal oxides both metal and oxygen ions can be exposed.

Allylic (amm)oxidation (the selective (amm)oxidation of olefins at the allylic position) represents a substantial contribution to the production of important organic chemicals by heterogeneous oxidation (1–5). However, little is known about vinylic ammoxidation of olefins in this context. This study focuses on the characterization of different γ-Al_2O_3-supported molybdenum oxide catalysts active in the direct formation of acetonitrile from ethylene and ammonia. No molecular oxygen was added to the reaction stream in order to study the reactivity of different types (if present) of lattice oxygen and to exclude surface reoxidation effects. Two different catalyst pretreatments were applied: heating in a flow of diluted oxygen (calcination) and heating in a flow of diluted hydrogen. This was to induce different concentrations of lattice oxygen and probably resulting in different molybdenum structures on the alumina surface. Previous experiments showed an unusual profile of acetonitrile formation as a function of time on stream which is schematically shown in Fig. 1 (6). Three regions of interest could be distinguished: a semi-steady-state, a transition period, and a steady state. Characteristic for the semi-steady state was a constant formation of acetonitrile, whereas the selectivity to other products was changing. Other products for calcined catalysts were water and CO_2, and water, hydrogen,

[1] To whom correspondence should be addressed: DSM Research, P.O. Box 18, 6160 MD Geleen, The Netherlands. E-mail: i.peeters@research.dsm.nl.

0021-9517/98 $25.00

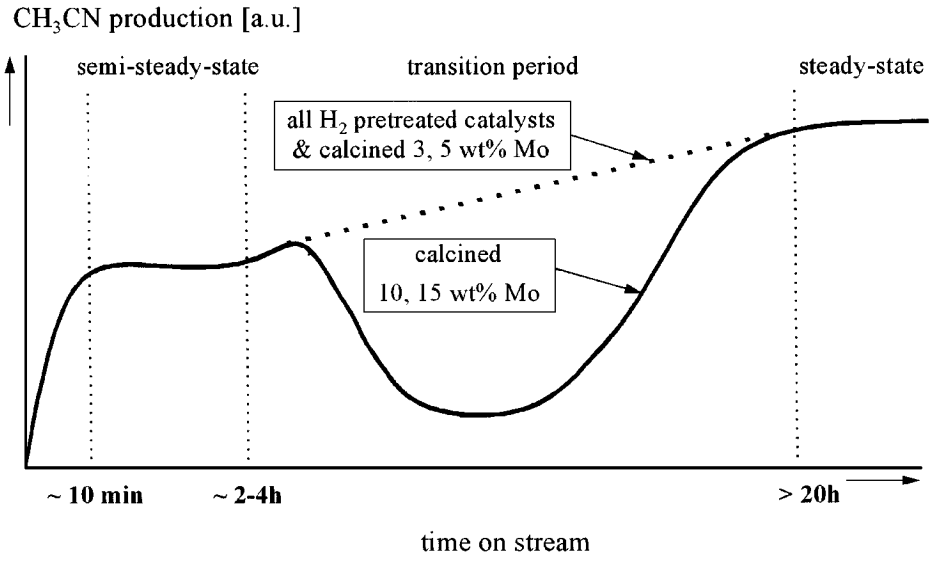

FIG. 1. A schematic profile of the formation of acetonitrile on various Mo/γ-Al_2O_3 catalysts as a function of time on stream. Flow 20 Nml/min: ethylene 7 μmol/min; ammonia 9 μmol/min; diluent helium; temperature between 350 and 500°C; 1.0 g of catalyst.

CO, methane, and ethane when pretreated with hydrogen. Since the product distribution and activity varied strongly with the different pretreatments applied, it was concluded that the reaction is highly structure-sensitive in this regime. When calcined, the catalysts were very selective but not very active. Hydrogen pretreated catalysts were very active but less selective. The performance during the transition period appeared to be dependent on the Mo content and catalyst pretreatment. Calcined catalysts with molybdenum content of 5 wt% or less and all catalysts pretreated with hydrogen showed a gradual increase in activity and acetonitrile formation (dotted line in Fig. 1). However, the calcined 10 and 15 wt% Mo catalysts showed a nongradual increase in both acetonitrile formation (solid line in Fig. 1) and activity. The conversion went through a maximum, forming hydrogen, nitrogen, methane, ethane, and CO, while the acetonitrile formation went through a minimum. When reaching the steady state, the yield of acetonitrile had increased 2 to 3 times for all catalysts, compared to the semi-steady state. The formation of hydrogen, nitrogen, and methane had decreased, whereas no CO formation was observed. It was concluded (6) that two routes for the formation of acetonitrile exist: one with the release of water as in the ammoxidation mechanism and the other with the release of hydrogen and co-production of ethane, resulting in oxidative ammonolysis. The two mechanisms operate simultaneously in the semi-steady state on hydrogen pretreated catalysts, whereas on calcined catalysts acetonitrile is formed only via ammoxidation. In the steady state, acetonitrile is only formed via oxidative ammonolysis, independent of the catalyst pretreatment.

To study structure–activity relationships, physical characterization of the catalyst in various conditions is needed. Since no single characterization technique is sufficient in providing all the information required, a well-chosen combination of several techniques must be applied. This study contains the results of several physical characterization techniques used to elucidate the structure–activity relationships existing in the oxidative ammonolysis of ethylene to acetonitrile over supported molybdenum catalysts. The characteristics, possibilities, and limitations of the applied techniques (X-ray diffraction, high resolution electron microscopy, X-ray photoelectron spectroscopy, and low-energy ion scattering) will be discussed in more detail below.

X-ray diffraction (XRD) is a characterization technique that can identify large three-dimensional crystallites. Although it is a very powerful tool to probe for the presence of crystalline phases, the detection limit is a minimum crystal size of approximately 4 nm (7) and two-dimensional metal oxide overlayers cannot be detected by XRD. Thus, when applied to a catalytic system, the absence of an XRD signal may be due to highly dispersed small crystallites, a low concentration of crystallites, or to the presence of a two-dimensional metal oxide overlayer, which is usually the case for supported catalysts with a low coverage. On the other hand, the presence of an XRD signal confirms that large crystallites are present.

A powerful technique to estimate particle size is high resolution electron microscopy (HREM). Combined with energy dispersive X-ray analysis (EDX), which gives the bulk composition of a restricted area, important parameters, such as the presence of impurities, dispersion, and morphology of the active phase, can be determined. The detection limit for small particles on a support is approximately 5 Å. The information obtained by XRD and TEM

concern large three-dimensional structures present in the catalyst. In a catalysis it is of great importance to know what kind of structures exist on the surface on an atomic level. So, a technique is required to identify the chemical environment and valency of the active phase.

X-ray photoelectron spectroscopy (XPS) supplies information on the elements present in the sample, as well as on their valency and chemical environment. Its analysis depth is about 50 Å, so several atomic layers are involved, rather than only the surface atoms. In order to obtain quantitative information on the concentration profile of the active phase in the catalyst or the particle size of the deposited material, a number of models have been proposed to predict XPS intensities for catalysts (8–12). In this study, the ratio of the molybdenum and aluminium signals is used as a tracer for changes in dispersion. With the Kuipers model (9) the Mo signal is calculated for an ideally dispersed molybdenum phase on γ-Al_2O_3. This way, the calculated ratio can be compared with the measured value. Although XPS can supply a large amount of information on the structure and valency state of the molybdenum phase, no estimation can be obtained on the distribution of the atoms positioned at the outermost layer. Since this layer is involved in the catalytic reaction, it is of great interest to apply a technique which can probe this layer.

Low-energy ion scattering (LEIS) is an extremely surface sensitive technique, enabling the selective analysis of the outermost atomic layer. In catalysis research, the analysis of this layer can be of great importance, since it is precisely this layer which is directly involved in the catalytic reaction. When applied to "real" catalysts, LEIS can supply information on structure, composition, and dispersion of the active material. Also, the effects of thermal treatment, adsorption/desorption, and reduction/oxidation can be studied (13).

Besides characterization of different pretreated fresh catalysts, used catalysts were also analyzed. The information obtained with these characterization techniques made it possible to elucidate structure–activity relationships in the heterogeneous reaction of ethylene with ammonia over supported molybdenum catalysts.

EXPERIMENTAL

1. Catalyst Preparation and Testing

The catalysts were prepared by incipient wetness impregnation of a commercial γ-Al_2O_3 (Akzo/Ketjen 000 1.5E; BET surface area 205 m^2/g and pore volume of 0.55 ml/g). A sieve fraction of 250–500 μm was used. Molybdenum was added from an aqueous solution of ammonium heptamolybdate-tetrahydrate (AHM, $(NH_4)_6Mo_7O_{24} \cdot 4H_2O$ obtained form Merck, p.a. quality) of 0.73, 1.23, and 1.90 g/ml, dependent on the Mo content required (3, 5, and 7.5 wt%, respectively). After impregnation the batch was heated slowly in air to 110°C overnight. Subsequently, the batch was heated in a flow of 20 Nml/min (where Nml stands for ml normalized to 273.15 K and 1 atm) of artificial air to 500°C and held there for 1 h. Batches containing 3, 5, 10, and 15 wt% molybdenum were prepared. Since the solubility of AHM is limited, the 10 and 15 wt% Mo catalysts were prepared by two subsequent steps of impregnation for 5 and 7.5 wt% Mo, respectively, according to the method described above.

The apparatus used for catalytic tests operated under atmospheric pressure. The catalyst bed was fixed between quartz wool plugs, and the remaining empty space in the reactor was filled with splinters of quartz to enhance plug flow. The reactor effluent was monitored on-line by a quadrupole mass spectrometer (Balzers QMG-420) for analysis of hydrogen (m/e = 2), water (m/e = 18, 17), ammonia (m/e = 17, 16), methane (m/e = 16, 15), ethylene (m/e = 27, 26), ethane (m/e = 30), acetonitrile (m/e = 41), CO_2 (m/e = 44). Organic compounds methane, ethylene, ethane, propane, acetonitrile, propinitrile, and acrylonitrile were analyzed quantitatively by introducing a sample into a Hewlett Packard 5890A gas chromatograph equipped with a Poraplot Q column, 10 m × 0.32 mm ID, and flame ionization detector (FID). Compounds, such as CO and CO_2, were quantitatively analyzed by introducing a sample into a Porapak N column, 6 ft × 3 × 2 mm (ED × ID) 80/100 mesh, equipped with a thermal conductivity detector (TCD) (14).

Experiments were done with an exact amount of 1.0 gram catalyst. Prior to reaction a reductive or an oxidative treatment was applied. The reductive treatment consisted of heating the catalyst in a 10 vol% hydrogen in helium flow of 20 Nml/min to 650°C, followed by an isothermal period of 24 h, whereas oxidative treatment (calcination) consisted of heating in a 10 vol% oxygen in helium flow of 20 Nml/min to 550°C, followed by an isothermal period of 24 h. The total flow was kept at 20 Nml/min and reaction temperatures were tested between 350 and 550°C. The reaction stream consisted of 1 vol% ammonia (9 μmol/min) and 0.8 vol% ethylene (7 μmol/min) in helium. All gases were purified by molsieves to remove water and by BTS catalysts to remove oxygen. A mixture of 1 vol% ethylene in helium (99.9% quality) and pure ammonia (99.96% quality) were provided by Hoekloos and used without purification.

2. X-Ray Diffraction

Powder diffraction patterns were collected on a Philips PW 7200 X-ray powder diffractometer using Cu-Kα radiation. A step scan mode was applied of 1°/1000 s. The catalyst was crushed and stored in a nitrogen atmosphere before pressing an amount in a sample holder.

3. High Resolution Transmission Electron Microscopy

Transmission electron micrographs were obtained by using a Philips CM 30 ST electron microscope with a field

emission gun as the electron source, operated at 300 kV. The samples of used catalysts were prepared by closing the reactor, after flushing and cooling the catalyst in a helium flow. Subsequently, the reactor was introduced into a nitrogen-filled glove box, where the catalyst was stored. Samples were mounted on a microgrid carbon polymer supported on a copper grid by placing a few droplets of a suspension of ground sample in ethanol on the grid, followed by drying at ambient conditions. For used catalysts, this procedure was also performed in a nitrogen filled glove-box.

4. X-Ray Photoelectron Spectroscopy

The X-ray photoelectron (XPS) spectra were recorded on a VG ESCALAB 200 spectrometer equipped with a standard dual X-ray source, of which the Al Kα part was used, and a hemispherical analyzer, connected to a five-channel detector. The background pressure during data acquisition was kept below 10^{-7} mbar. Measurements were performed at 20 eV pass energy, and charging was corrected for using the C 1*s* signal at 284.5 eV as a reference. Since also used catalysts were submitted to XPS analysis, different carbon species can be present on the surface. The correctness of this method was confirmed by comparing the charging using the Al 2*p* and O 1*s* signals, with binding energies at 74.0 and 531.0 eV ($\pm$0.2 eV), respectively. Spectra were fitted with the vacuum generators scientific (VGS) program fit routine. A Shirley background subtraction was applied and Gauss–Lorentz curves were used for the fits. The samples were prepared by closing the reactor, after flushing and cooling the catalyst in a helium flow. Subsequently, the reactor was introduced into a nitrogen-filled glove box. The catalyst was crushed and mounted on an iron stub carrying an indium film. The sample was placed in a vessel filled with nitrogen for transport to the spectrometer and no pretreatment was applied prior to measurement.

5. Low-Energy Ion Scattering

The newly developed ERISS was used as the ion scattering apparatus. The analyzer of the ERISS is approximately 1000 times more sensitive than a conventional one. In this apparatus ion doses can be reduced to such a low level that the damage of the surface is negligible, thus enabling the performance of static LEIS. Using a effective spot area of 3×3 mm it is possible to obtain spectra with total ion doses less than 10^{12} ions/cm^2. The time needed for a full energy spectrum is typically 6 min. To prevent charging of insulating materials, a neutralizer was used to spray low-energy electrons to the sample.

Samples were prepared by pressing an amount of ground sample with a load of 1600 kg into a tantalum cup ($\varnothing$ 1 cm) and placed into the pretreatment chamber, which is connected to the main UHV chamber. Pretreatment of fresh catalysts consisted of heating overnight in either 0.5 bar of oxygen to 275°C, or in 0.5 bar of hydrogen to 240°C in order to remove adsorbed water, oxygen, and CO_2. The used catalysts and pure MoO_2 were heated in 0.5 bar of hydrogen to 100°C for 2 h. Pure MoO_3 and $Al_2(MoO_4)_3$ were heated in 0.5 bar of oxygen to 160°C for 2 h. After evacuating (until $p < 10^{-6}$ mbar) and some cooling, the sample was transported to the main chamber for analysis.

Successive spectra were obtained from scattering 3 keV He^+ using ion doses of 10^{14}, 7.5×10^{14} or 2.5×10^{15} ions/cm^2. Subsequent spectra were basically identical, confirming that the ion dose applied for the measurement did not influence the measurement. To avoid shielding by adsorbed species, the samples were transported to the main chamber while still hot after a heat treatment with hydrogen. For reference compounds, pure MoO_2 and $Al_2(MoO_4)_3$ were obtained from Johnson Matthey (p.a. quality), and MoO_3 was obtained from Merck (p.a. quality).

Since the use of absolute intensities is often complicated by the difficulty in reproducing the experimental conditions with various samples, a method to ratio the peaks of interest to an internal standard is usually applied. Oxygen is often used as an internal standard for supported oxide catalysts, since the intensity of oxygen for these systems is suggested to remain relatively constant (15–17). However, if the oxygen coverage on the various samples changes (due, for example, to different crystal structures), one may derive incorrect results. Evidence of this phenomenon can be found in Table 2, comparing the oxygen signals of MoO_2 and MoO_3; the ratio is not 2 : 3 but 0.69 : 0.78 (= 2 : 2.3). We have developed an experimental procedure which proved to by very successful in using the absolute intensities quantitatively. To do this properly, specific conditions need to be fulfilled. The method of collecting spectra must be reproducible, the use of realistic model compounds as standard is required and the performance of static LEIS, which implies that damage caused by the ion bombardment and preferential sputtering is negligible. As a result of this, light elements, such as adsorbed hydrogen, carbon, and nitrogen species, are not removed very easily by sputtering. An important uncertainty remains, if the porosity of the sample can influence the absolute signals. A short-range ordering is needed to compare signals of different samples properly. The γ-Al_2O_3 support has a BET specific surface area of 200 m^2/g, whereas the reference compounds this concerns 1–2 m^2/g. With this in mind, a reliable use of absolute intensities to calculate the coverages of the support with the active material is obtained, which is presented in this paper.

RESULTS AND DISCUSSION

1. High Resolution Transmission Electron Microscopy

In this study, bright field transmission electron microscopy (TEM) was applied to estimate the particle size

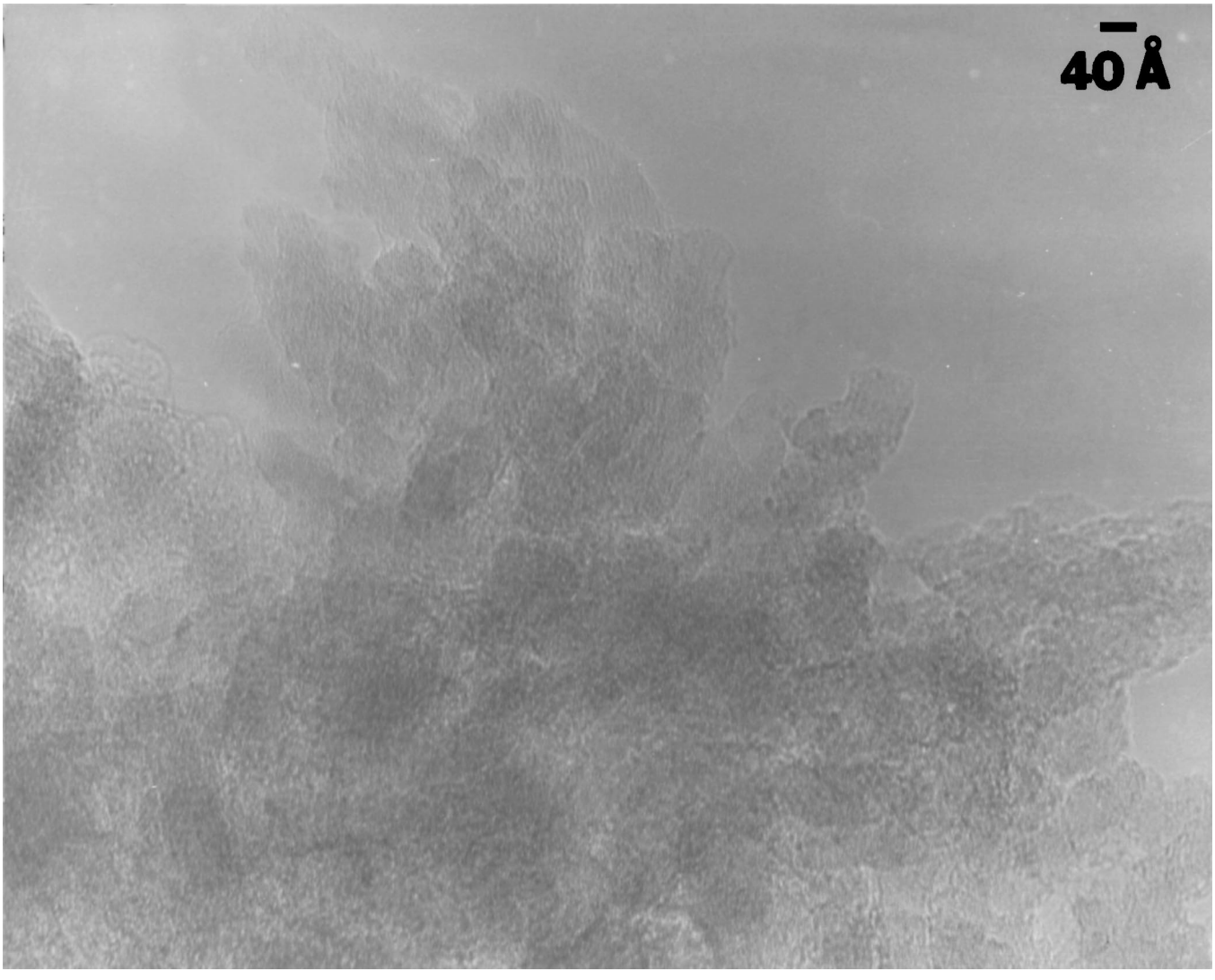

FIG. 2. HR-TEM image of a calcined 5 wt% Mo catalyst after 24 h on stream at 450°C. The polycrystalline phase correlates with γ-Al_2O_3; no Mo particles are visible on the alumina surface.

of the molybdenum phase and to probe for crystallinity. Figure 2 shows a TEM image of a calcined 5 wt% Mo catalyst after reaching the steady-state. All fresh and all used catalysts studied here showed images identical to Fig. 2. The polycrystalline structure could be correlated to γ-Al_2O_3. No molybdenum oxide particles were visible on the alumina surface, implying that the particle size was less than the detection limit of 5 Å. EDX analysis showed a molybdenum to aluminium signal ratio which was constant over different areas in one sample and increased with increasing molybdenum content of the sample. This also implies that the samples were very homogeneous.

For freshly calcined catalysts with a molybdenum content exceeding 5 wt% Mo, large crystalline particles with a different structure and composition appeared (see Fig. 3). The size of these crystals (>200 Å) indicates that the molybdenum was not adsorbed inside the alumina pores, but were formed separate from the support. Two spacings were determined (5.4 and 8.2 Å) of which the first could be assigned to $Al_2(MoO_4)_3$ (18).

After submitting the freshly calcined catalysts containing a high amount of molybdenum (>5 wt% Mo%) to the reaction, large crystals were observed with HR-TEM as well. This is shown in Fig. 4, which presents an image of the used calcined 15 wt% Mo catalyst. The size of the dark crystal is approximately 165 × 225 Å. The spacings measured (3.42 and 2.42 Å) coincide with those for MoO_2 (19).

2. *X-Ray Diffraction*

Figure 5 shows XRD spectra of several calcined, hydrogen pretreated and used catalysts. The spectra of the calcined 3 wt% Mo, the hydrogen pretreated and the used 3, 5, and 10 wt% Mo catalysts showed a spectrum

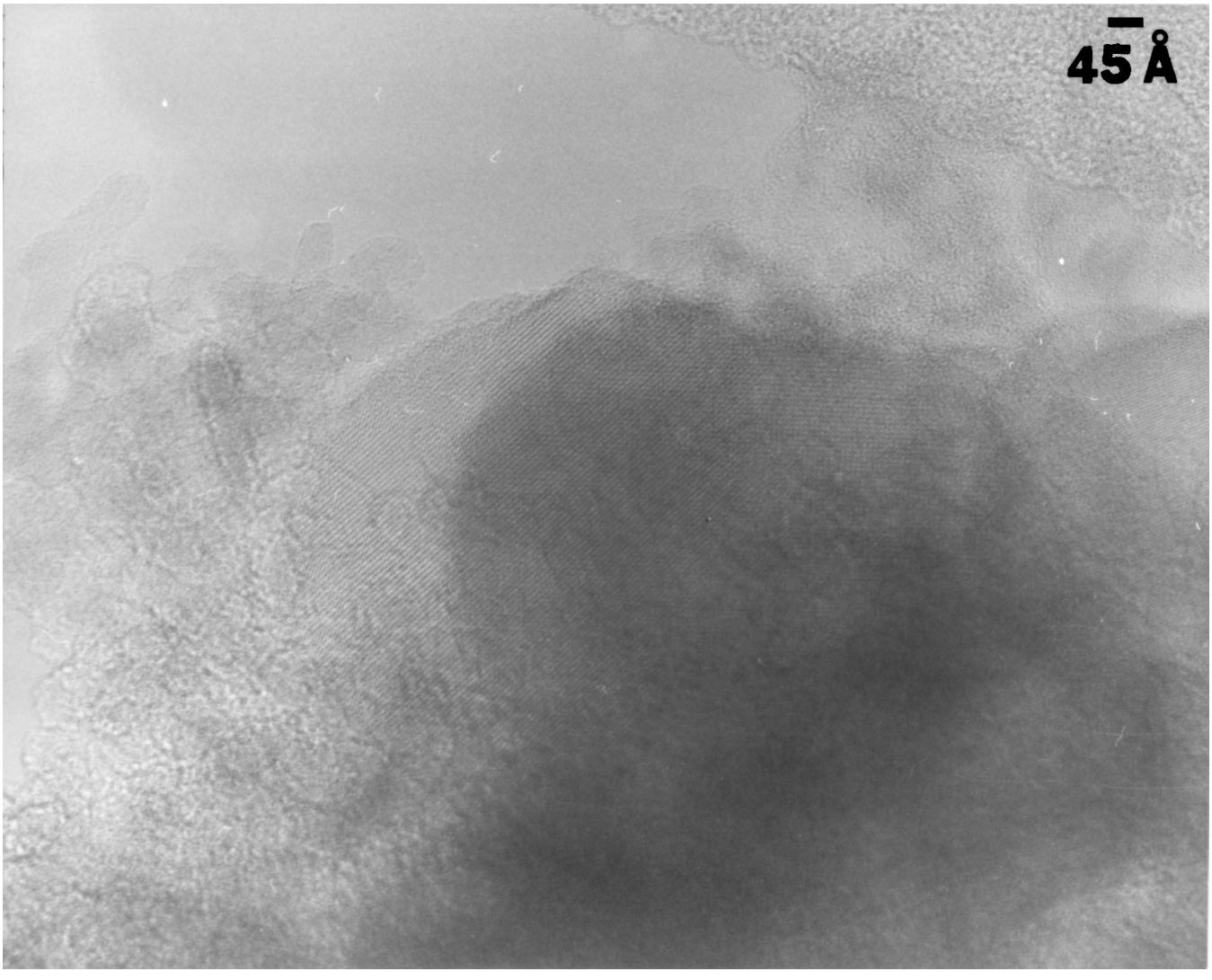

FIG. 3. HR-TEM image of a fresh calcined 15 wt% Mo catalyst. The size of the crystal is >200 Å. A spacing was measured of 5.4 Å which can be ascribed to $Al_2(MoO_4)_3$ (18).

similar to that of the bare support (a) and the calcined 5 wt% Mo catalyst (b) and are therefore omitted. The fact that no other signals appeared implicates that these catalysts contained very small crystallites or the molybdenum phase is amorphous or two-dimensional. After calcination, the 10 wt% Mo catalyst showed traces of a crystalline phase (c), whereas clear signals appeared at 15 wt% Mo (d). These signals (marked with $*$) could be ascribed to $Al_2(MoO_4)_3$ (18). The observation of chemical interaction of alumina and molybdate is in agreement with the work of Giordano *et al.* (20), where $Al_2(MoO_4)_3$ was observed on MoO_3/γ-Al_2O_3 catalysts containing more than 20 wt% MoO_3 after calcination at 700°C. The aggregation of free MoO_3 was excluded, except for the 30 wt% MoO_3/γ-Al_2O_3 catalyst. It was suggested that $[MoO_6]$ in the octahedral vacancies is the precursor of $Al_2(MoO_4)_3$ and that the formation of this stable phase is slow. The formation of $Al_2(MoO_4)_3$ was already observed by Sonnemans and Mars (21) and Asmolov and Krylov (22).

When freshly pretreated with hydrogen, no crystallinity is observed up to 15 wt% Mo (Fig. 5e), and the signals appearing in the spectrum of the 15 wt% Mo catalyst are small. The peaks indicated with # in Fig. 5 can be assigned to MoO_2 (19). This implies that during a hydrogen pretreatment the structure of $Al_2(MoO_4)_3$ is altered, and a different stable molybdenum structure is formed, namely MoO_2.

It is expected that not only a change in the molybdenum structure can occur during hydrogen pretreatment but also during reaction. When all oxygen pretreated catalysts were analyzed by XRD after reaching the steady state, only the 15 wt% Mo showed clear signals of MoO_2 (f). The spectrum of the hydrogen pretreated used 15 wt% Mo was similar to its calcined analogue. Comparing the XRD spectra (e) and (f) in Fig. 5, it can be concluded that even after a

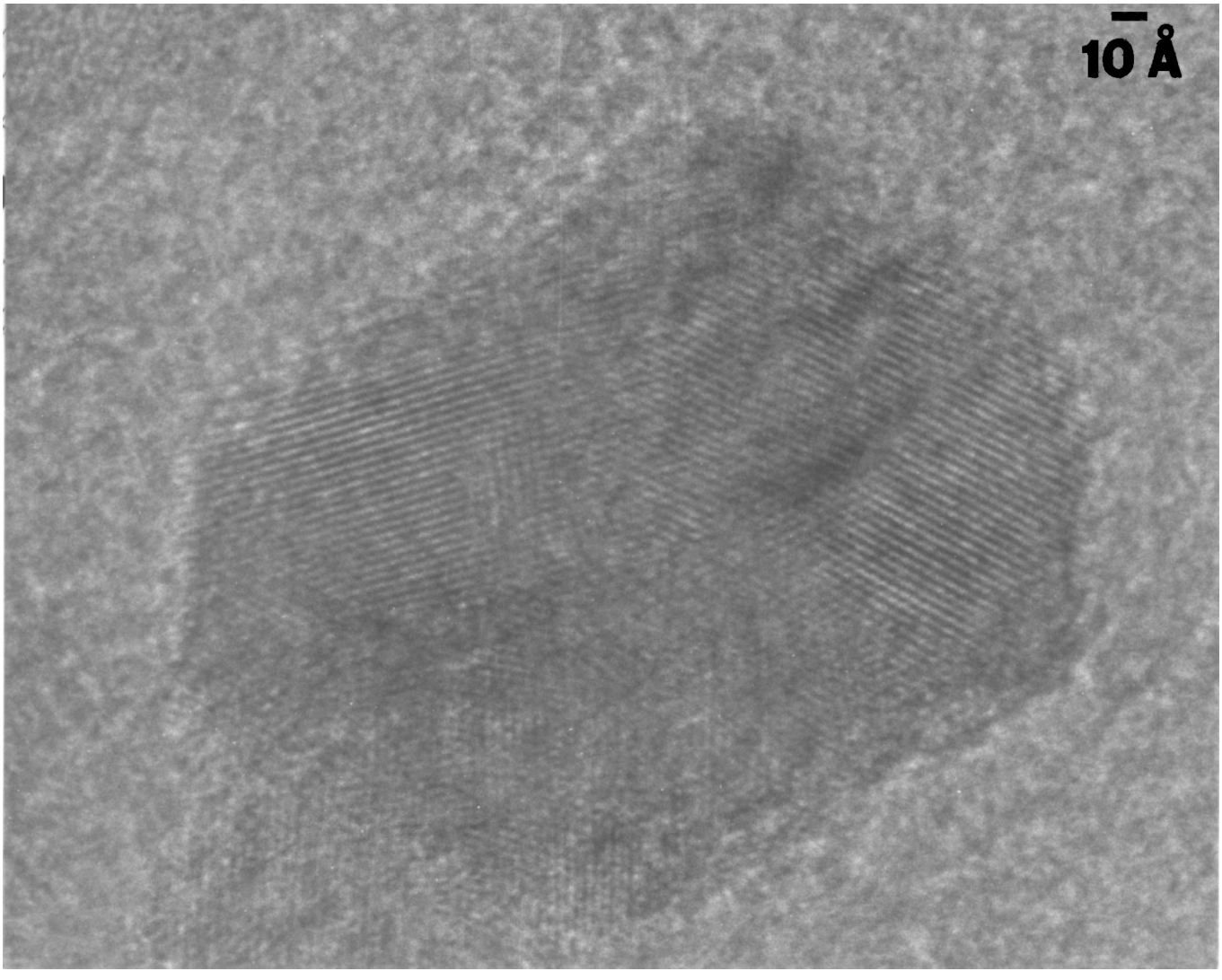

FIG. 4. HR-TEM image of a calcined 15 wt% Mo catalyst after 24 h on stream at 450°C. The size of the crystal is approximately 165 × 225 Å. Spacings were measured of 2.42 and 3.42 Å which can be ascribed to MoO_2 (19).

vigorous reductive treatment, the catalyst morphology is altered further under reaction conditions. The presence of large $Al_2(MoO_4)_3$ crystals in freshly calcined catalysts with a high Mo content can explain the unusual catalytic profile of these catalysts, where during the transition period of high activity and low selectivity the structure is converted to large MoO_2 crystals. The absence of large $Al_2(MoO_4)_3$ crystals in freshly reduced catalysts explains their gradual catalytic profile in the transition period.

The maximum adsorption capacity of the alumina used in this study is approximately 8–9 wt% Mo (23). The overall trend observed is that when this maximum adsorption capacity is exceeded, the excess of molybdenum is used for the formation of large crystals. Dependent on the catalyst pretreatment these crystals are either $Al_2(MoO_4)_3$ or MoO_2.

3. *X-Ray Photoelectron Spectroscopy*

In this study, the ratio of the molybdenum and aluminium signals is used qualitatively as an indicator for changes in the dispersion of molybdenum. When the molybdenum added spreads ideally on the support surface, this ratio will not differ significantly from the theoretical ratio. When particles agglomerate, a part of the molybdenum is invisible for XPS and less alumina will be covered, resulting in a lower ratio than theoretically predicted.

The position of the binding energy of an element not only reveals the valency state, but usually, also, its chemical environment. This study focuses on the position of the Mo $3d_{5/2}$ signal.

Changes in dispersion. The ratio of the intensities of the XPS signals of Mo 3*d* and Al 2*p* for fresh catalysts is plotted

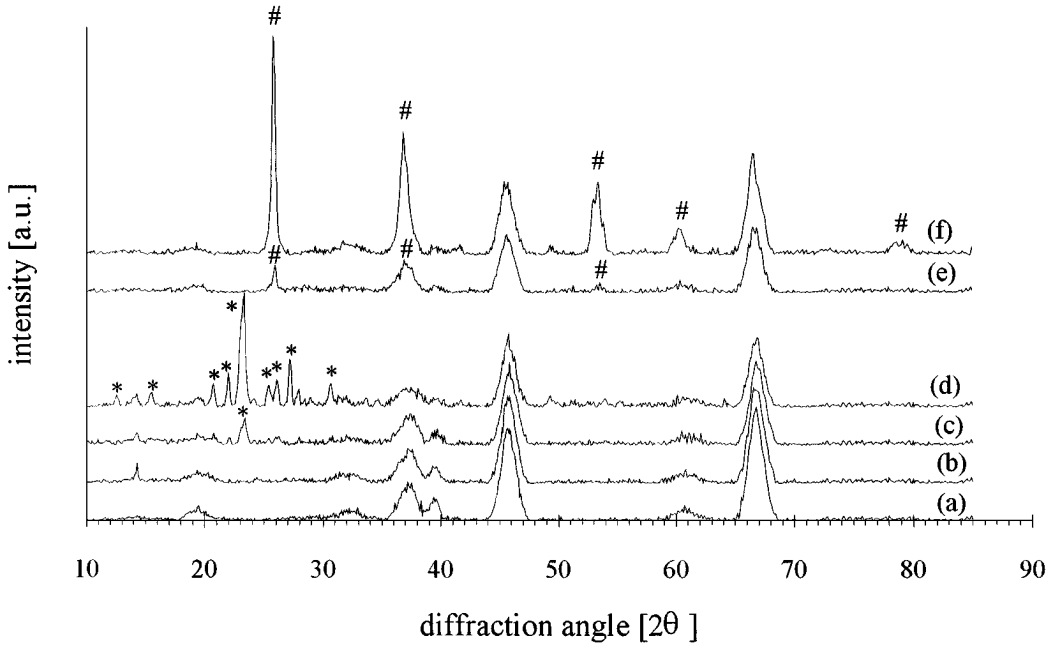

FIG. 5. XRD spectra of γ-Al_2O_3 (a); fresh calcined catalysts with 5 wt% Mo (b); 10 wt% Mo (c); 15 wt% Mo (d); a fresh hydrogen pretreated catalyst with 15 wt% Mo (e); and a calcined catalyst used for 24 h at 450°C (f). The ∗ indicates typical lines for $Al_2(MoO_4)_3$ (18); the # indicates typical lines for MoO_2 (19).

in Fig. 6 (solid lines). Overall, the ratio was higher for the oxygen pretreated catalysts than for those after a reductive treatment, although the difference is small at low molybdenum content. Up to 5 wt% Mo, a similar increase was observed independent of the pretreatment applied. This supports the idea of the presence of isolated small Mo particles, which are difficult to reduce and resistant to aggregation, resulting in only small changes in dispersion at these low coverages. At higher molybdenum content, however, the ratio

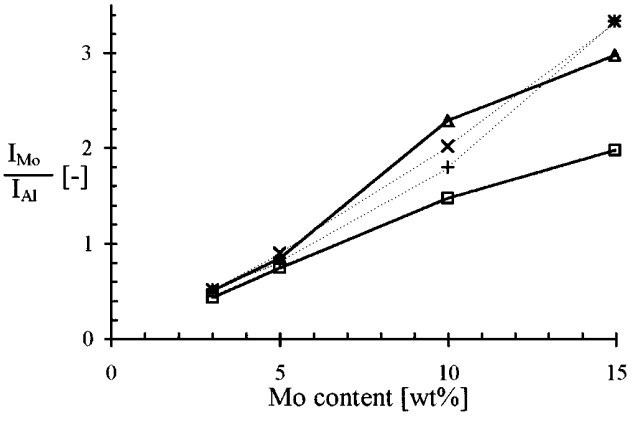

FIG. 6. Intensity ratio of the XPS signals of Mo 3*d* and Al 2*p* as a function of Mo content and catalyst pretreatment. The symbols △ and □ represent measured values for freshly calcined and hydrogen pretreated catalysts. The symbols + and × represent calculated values according to the model applied (12).

for oxygen pretreated catalysts is substantially higher than for the hydrogen pretreated ones, the latter showing a linear increase of the I_{Mo}/I_{Al} ratio as a function of molybdenum content. Apparently, at higher coverages, the molybdenum is better dispersed when calcined than when reduced.

A theoretical I_{Mo}/I_{Al} was calculated by using Kuipers model (9), in which the catalyst is represented by small surface species with a random orientation with respect to the analyzer. The physical upper limit of the intensity of the molybdenum signal was calculated, using the molybdenum phase (4.7 and 6.5 g/cm^3 for MoO_3 and MoO_2, respectively), the concentration of the dispersed compound (g/100 g catalyst) and the measured intensities and binding energies of aluminium (Al 2*p*, 74 eV) and molybdenum (Mo 3*d*, 230 eV). The photoelectric cross sections were estimated according to Scofield (24) and a Seah factor for inorganic compounds of 0.72 (25) was applied. A theoretical I_{Mo}/I_{Al} was calculated from the calculated physical upper limit of the molybdenum signal and the aluminium signal and is represented by the dotted lines in Fig. 6. For the freshly calcined catalysts, the theoretical line and the measured line agree well up to 10 wt% Mo, indicating an optimum dispersion of the molybdenum. When pretreated with hydrogen, these lines agree up to 5 wt%, which implies a highly dispersed molybdenum phase which aggregates at higher Mo content to larger particles upon reduction.

Changes in valency state. Besides changes in dispersion, also changes in the valency state of molybdenum are expected upon hydrogen pretreatment. To identify

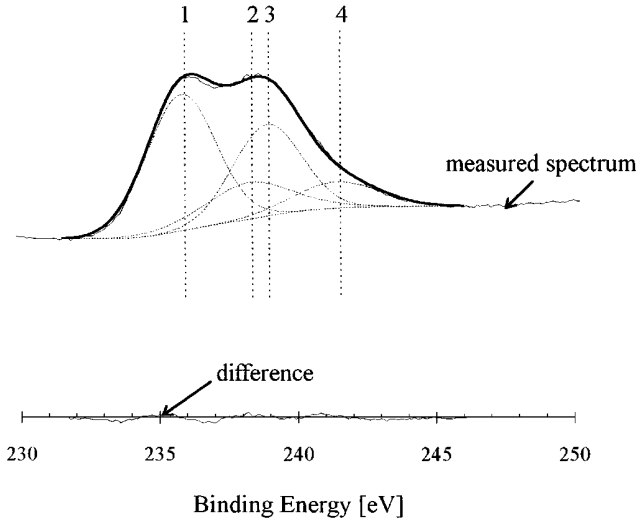

FIG. 7. The deconvolution of the Mo 3*d* spectrum of a calcined 10 wt% Mo catalyst after 24 h on stream. Charging of 6.2 eV was not corrected for. The splitting of the 3*d* (into 3/2 and 5/2) is 3.13 eV, whereas the area ratio $3d_{3/2}:3d_{5/2}$ must be 2 : 3. Curve 1, Mo(IV) Mo $3d_{5/2}$; curve 2, Mo(VI) Mo $3d_{5/2}$; curve 3, Mo(IV) Mo $3d_{3/2}$; curve 4, Mo(VI) Mo $3d_{3/2}$.

different valency states of an element, the XPS spectrum must be deconvoluted. As an example, the Mo 3*d* spectrum of a calcined 10 wt% Mo catalyst after 24 h on stream is shown in Fig. 7, with the deconvolution curves of the Mo $3d_{5/2}$ and Mo $3d_{3/2}$ signals originating from Mo(IV) and Mo(VI) (see Table 1 for the exact value of the binding energies).

When freshly calcined, only hexavalent molybdenum (Mo(VI)) was detected, which has a Mo $3d_{5/2}$ peak at a binding energy of 232.5 eV. Figure 8 depicts the Mo 3*d*

TABLE 1

XPS Mo $3d_{5/2}$ Binding Energies of Molybdenum in Different Valencies and Chemical Environments

	Mo $3d_{5/2}$ (eV)
Mo(II)	228.4 (26)
Mo(IV) (type 1) in MoO_2	228.4 (27, this work)
Mo(IV) (type 2) in MoO_2	229.6 (27, this work)
Mo(V)	230.5 (this work)
Mo(VI) in MoO_3	232.5 (28, this work)

signals for freshly hydrogen pretreated catalysts. Indeed, after hydrogen pretreatment other valency states of molybdenum appeared, besides Mo(VI). The 3 wt% Mo catalyst showed very little reduction. The line broadening suggests the presence of Mo(V) species, which show a $3d_{5/2}$ signal at approximately 230.5 eV. Although the presence of lower valency states than 4+ could not be determined properly, the position of the Mo $3d_{5/2}$ signal at 228.4 eV can very well be attributed to Mo(II) (26). Since the stability of Mo(II) in oxidic systems is very low, its formation is not likely to occur in the catalytic systems considered. The overall amount of reduction increased at increasing molybdenum content to a maximum at 10 wt% Mo. By deconvoluting the 3*d* curve, an amount of Mo(IV) could be estimated, which is shown in Fig. 9A, by the white bars for fresh catalysts. The 5 wt% Mo catalyst contained about 70% Mo(IV), whereas on the 10 wt% Mo catalyst even 80% Mo(IV) was observed. The amount of Mo(IV) in the 15 wt% Mo catalyst was only 45%, whereas the position of the $3d_{5/2}$ signal was shifted to 229.6 eV, compared to the binding energy at 228.4 eV found for the 10 wt% Mo catalyst (see Table 1). This suggests a

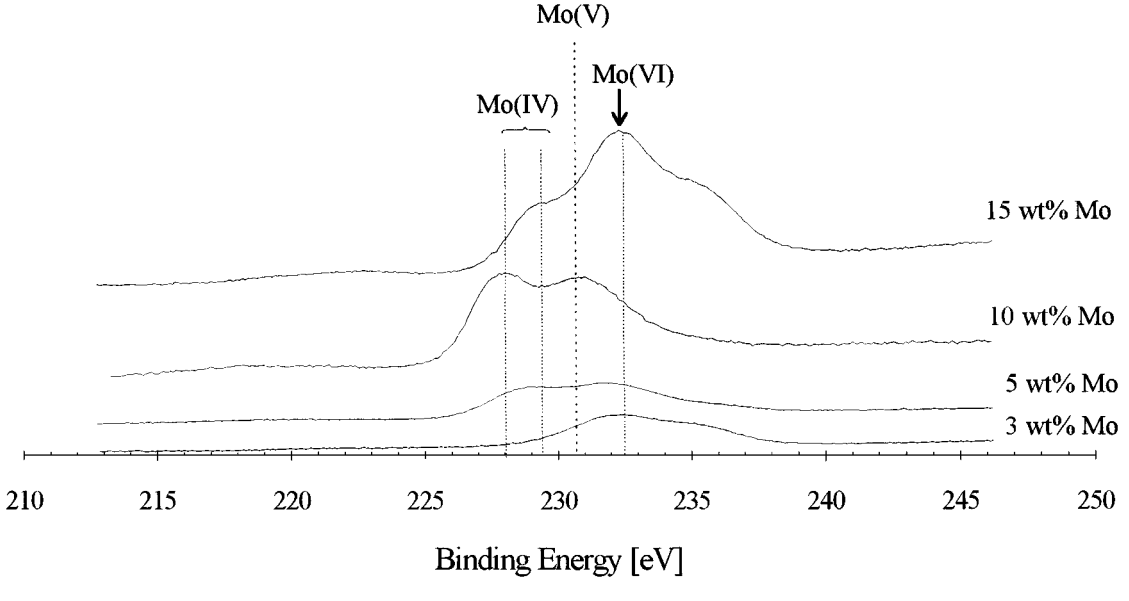

FIG. 8. XPS spectra of the Mo 3*d* signal of catalysts with various molybdenum content after hydrogen pretreatment for 24 h at 650°C. The dotted lines indicate the position of the Mo $3d_{5/2}$ signal.

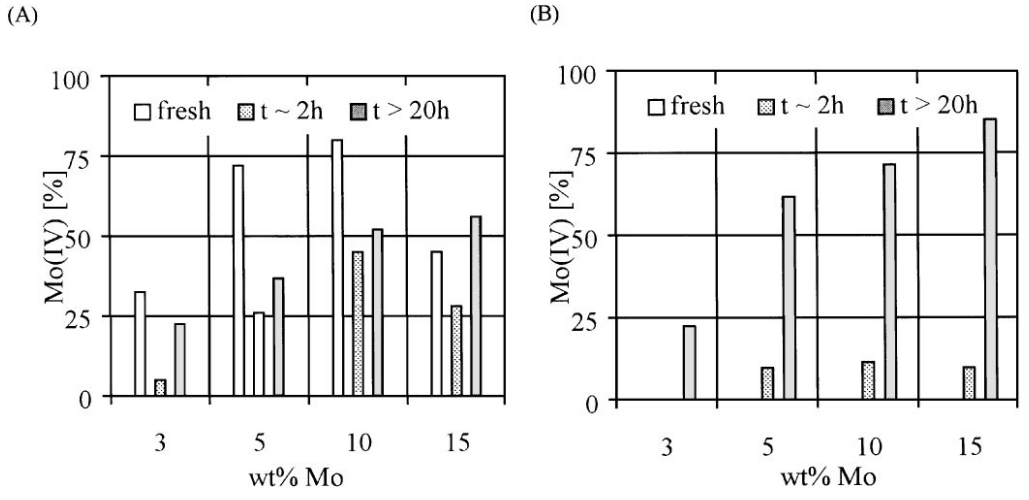

FIG. 9. Fraction Mo(IV) calculated from deconvoluting the Mo 3*d* signal for hydrogen pretreated (A) and calcined catalysts (B) fresh, □; at the semi-steady-state, ▨; and the steady-state period at 450°C, ■.

change in chemical environment, which will be discussed in the next section.

For XPS analysis of used catalysts the reaction was quenched at various times on stream. Figures 9A and B depict the percentage of Mo(IV) of fresh catalysts, in the period of semi-steady state and steady state of the reaction for the different pretreated catalysts as a function of molybdenum content. Although the hydrogen pretreatment induced a more reduced molybdenum surface (a higher amount of Mo(IV) compared to the used catalysts), not all reactive lattice oxygen was removed, since in all cases oxygen-containing products were observed prior to the steady state. It is remarkable that the amount of Mo(IV) decreased for hydrogen pretreated catalysts in the semi-steady state (Fig. 9A, dotted bars), compared to the fresh ones. During reduction with hydrogen the removal of lattice oxygen at the surface is faster than the transport of lattice oxygen to the surface, whereas under reaction conditions the diffusion of lattice oxygen to the surface is faster than removal by reaction. When freshly calcined, obviously no Mo(IV) is present in the fresh catalysts. During the semi-steady state period the amount of Mo(IV) appeared to be independent of the Mo content (Fig. 9B; dotted bars), whereas an increase with increasing Mo content was observed after reaching the steady-state (Fig. 9B, striped bars). It can be concluded from the high amounts of Mo(IV) on the calcined catalysts at steady state that, starting with a highly dispersed freshly calcined precursor, the catalyst surface can be further reduced by reaction than with a freshly hydrogen pretreated catalyst.

The increase of the yield of acetonitrile in the steady state compared to the semi-steady state cannot be attributed only to the increase of the amount of Mo(IV). Although the oxygen pretreated 5 wt% Mo catalyst yielded the highest amount of acetonitrile at steady state (6, 14), the largest amount of Mo(IV) was observed on the used oxygen pretreated 15 wt% Mo catalyst. Apparently, a well-dispersed calcined precursor is needed to obtain the best performance in the steady state, where both Mo(IV) and Mo(VI) species are present.

Chemical environment of the molybdenum. As an example, XPS spectra of the calcined 10 wt% Mo catalyst after various times on stream are shown in Fig. 10 (6, 14). For comparison, the spectra of pure MoO_2 and MoO_3 are included. A catalyst containing almost 100% Mo(VI) (see Fig. 10, after ~1.3 h) was not very active, but highly selective to acetonitrile. Before the yield started to decrease, some reduction of molybdenum was observed with XPS (after ~2.5 h, not shown in Fig. 10). Due to the large $Al_2(MoO_4)_3$ crystals present at high molybdenum content, the presence of a large amount of still-removable surface oxygen in a partly reduced catalyst (due to reaction) leads to very high activity, but only toward hydrogenation and the formation of methane, hydrogen, nitrogen, and CO. The latter is terminated at depletion of removable lattice oxygen.

It was suggested in the preceding section that the Mo $3d_{5/2}$ signal for hydrogen pretreated catalysts at 228.4 eV can very well be ascribed to Mo(II), implying a further reduction of the molybdenum. According to Haber *et al.* (27), Mo(IV) can exist in two forms: (1) represents isolated Mo^{4+} ions, whereas (2) constitutes Mo^{4+} ions forming pairs in clusters of edge-sharing octahedra, which may be considered as nuclei of a MoO_2 phase. The binding energy of Mo(IV) in form 1 is typical for Mo(IV) in MoO_2, whereas the binding energy of Mo(IV) in form 2 is Mo(II)-like. Since divalent molybdenum ions are known to be very unstable in oxidic systems, the appearance of the apparent oxidation number of 2+ must originate from Mo(IV) in form 2. After reaching the steady-state, the position of the Mo $3d_{5/2}$ signal of Mo(IV)

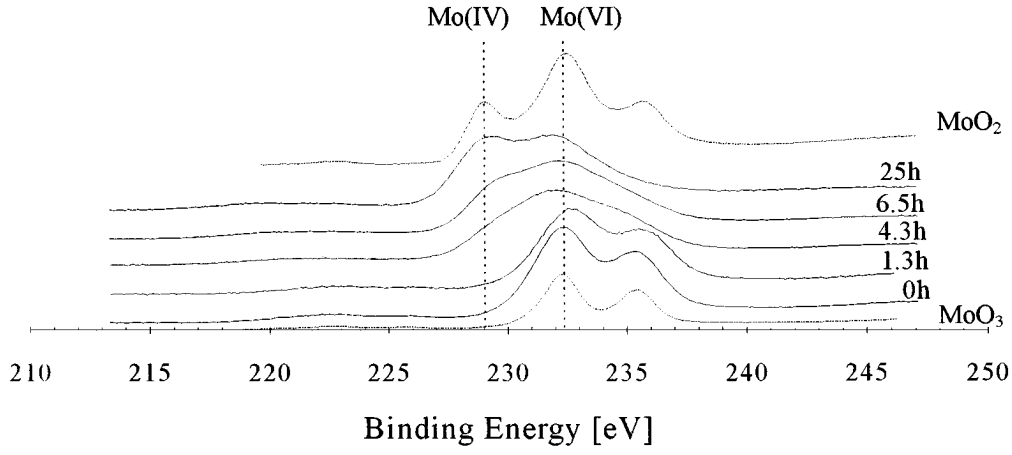

FIG. 10. XPS spectra of the Mo 3*d* signal of pure MoO_2, MoO_3, and a calcined 10 wt% Mo catalyst at various times on stream at 450°C.

for all catalysts was about 229.5 eV. In the literature, the Mo(IV) $3d_{5/2}$ signal at 229.5 eV is ascribed to Mo(IV) in a MoO_2 structure (28) (see Table 1). Since at steady state the catalyst has reached a chemical and structural equilibrium, it is concluded that surface MoO_2 is the active phase for the formation of acetonitrile in that period.

Other elements present on the molybdenum surface. When submitted to reaction, an increase of the C 1*s* peak was observed, compared to the fresh catalyst, suggesting that coke formation had occurred. Since the catalytic activity showed no indications of deactivation, this carbon could be removed by the reaction stream, or act as a reaction intermediate. Also, coke deposition on the alumina cannot be excluded. Nitrogen containing species are very difficult to detect by XPS, because of the low sensitivity towards nitrogen and the interference of the Mo $3p_{3/2}$ signal of Mo(VI). Only at higher molybdenum content and after long time on stream, the N 1*s* signal could be distinguished. From the binding energy at 398 eV it is concluded that atomic nitrogen is involved coupled to a carbon or (a) hydrogen atom(s). The formation of molybdenum nitrides, which would show a signal at a lower binding energy is excluded.

4. *Low-Energy Ion Scattering*

The freshly calcined catalysts showed already constant spectra after a low ion dose, indicating that the surface was not covered significantly by light elements. When a sample is pretreated with hydrogen, careful sputtering is necessary, until the signals present remain constant. Charging of insulating samples was prevented by a neutralizer.

Surface composition and corresponding structures. In Fig. 11 the LEIS spectra of γ-Al_2O_3 and freshly calcined

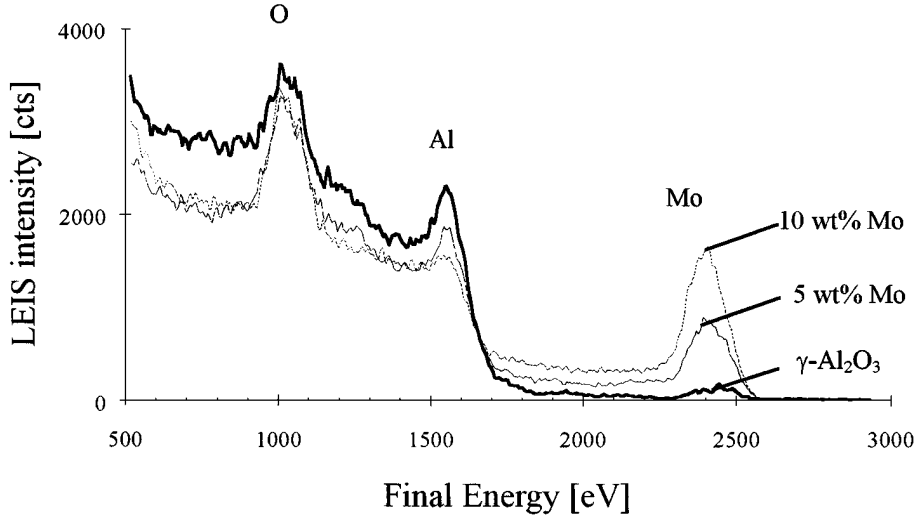

FIG. 11. LEIS spectra of 3 keV $^4He^+$ scattering from γ-Al_2O_3 and fresh calcined catalysts with various molybdenum contents. All spectra were taken after an ion dose of approximately 5×10^{14} ions/cm^2.

TABLE 2

The Ratio (r) of LEIS Signals of the Reference Compounds with Corresponding Absolute Areas (S) Normalized to an Identical Beam Current

Reference compound	Measured values	
	Ratio $r_{Al}:r_O:r_{Mo}$	Normalized areas $S_{Al}:S_O:S_{Mo}$
MoO_2	0 : 0.69 : 1	0 : 227 : 331
MoO_3	0 : 0.78 : 1	0 : 290 : 374
γ-Al_2O_3	1 : 1.10 : 0	106 : 120 : 0
$Al_2(MoO_4)_3$	1 : 9.65 : 13.42	20 : 195 : 271

catalysts with 5 and 10 wt% Mo are shown. In Tables 2 and 3 the data are shown for the reference compounds and the catalysts, respectively. It appeared that the surface of the support already contained a small amount of molybdenum corresponding to less than 1 wt%. The 5 wt% Mo catalyst showed a clear signal of molybdenum. At 5 wt% Mo, the amount of one-third of a monolayer (29) is added to γ-Al_2O_3, where the area of a Mo cluster is assumed to be 20 Å^2 (30). This is in agreement with the decrease of approximately 30% of the aluminium signal compared to the bare support (31). The freshly calcined catalyst containing 10 wt% Mo showed an increase of the Mo signal by a factor of 2, which can be expected when the molybdenum is well spread on the alumina surface, where it is easily detectable by LEIS. Brongersma *et al.* (32) observed a sudden decrease of the Al signal versus molybdenum content at 8 wt% MoO_3 (5.3 wt% Mo). At coverages exceeding 8 wt% MoO_3 the Al signal decreased linearly with increasing Mo content. The increase of the Mo signal was linear upto 19 wt% MoO_3 (12.7 wt% Mo). So, the catalysts studied here with LEIS (5 and 10 wt% Mo) are in the region where both the Al and Mo signals behave linearly.

To obtain more specific information about the atomic distribution on the surface and on the nature of the molybdenum phase on the alumina, the LEIS data were used quantitatively. Several compounds, which were expected to be present in the catalyst, were measured for reference purposes. A model was applied where the alumina surface is covered with one particular molybdenum structure. A schematic representation is shown in Fig. 12, where the γ-Al_2O_3 supports either MoO_3, $Al_2(MoO_4)_3$, or MoO_2 structures (A, B, and C, respectively). The surface can be considered to consist of support and a reference compound representing the active material. So, it must be possible to fit the measured signals of the catalyst by using a combination of the signals of support and the specific reference compound. This way the type of active phase can be identified and the coverage θ can be calculated, resulting in an estimation of the dispersion. The signals S measured on the catalyst originate partly from the support, resulting in an oxygen signal S_O^* and an aluminium signal S_{Al}^*, and from the active material, resulting in an oxygen signal S_O, molybdenum signal S_{Mo} and, if $Al_2(MoO_4)_3$ is modelled as active material, also an aluminium signal S_{Al}. The percentage of the alumina covered with molybdenum can be calculated by using the decrease in the aluminium signal of the catalyst compared with the bare support (31) or using the absolute molybdenum signals of the catalyst and the reference compound (33). However, when $Al_2(MoO_4)_3$ is present on the γ-Al_2O_3 surface, the aluminium signal contains a contribution of both support and active material (see Fig. 12B, S_{Al}^* and S_{Al}, respectively, where $*$ indicates a signal originating from the support). Subsequently, the oxygen signal can be calculated (34), which contains a contribution of the support and the molybdenum oxide (S_O^* and S_O, respectively), and compared with the measured value to check the reliability of the fit. The data of the reference compounds used are listed in Table 2. The experimental and calculated

TABLE 3

The Measured Ratios (r), Absolute Areas (S), Calculated Coverage θ, Total Oxygen Signal ($S_O + S_O^*$, Which Is Composed of the Oxygen Signal from the Support S_O^* and the Molybdenum Phase S_O) and Ratios with Corresponding Reference Compounds for Various Fresh Mo Catalysts

Catalyst	Measured		Calculated			Reference
	Ratio $r_{Al}:r_O:r_{Mo}$	$S_{Al}:S_O:S_{Mo}$	θ [%] (33)	$S_O + S_O^*$ (34)	$r_{Al}:r_O:r_{Mo}$ (35, 36)	
5 wt% Mo; calcined	1 : 2.07 : 1.41	75 : 154 : 105	28	168	1 : 2.20 : 1.41	MoO_3
			39	**149**	**1 : 2.11 : 1.41**	**$Al_2(MoO_4)_3$**
10 wt% Mo; calcined	1 : 4.15 : 4.79	44 : 180 : 208	56	215	1 : 4.84 : 4.79	MoO_3
			77	**178**	**1 : 4.43 : 4.79**	**$Al_2(MoO_4)_3$**
5 wt% Mo; reduced	1 : 1.30 : 0.54	84 : 109 : 45	14	150	1 : 1.47 : 0.54	MoO_2
			12	140	1 : 1.52 : 0.54	MoO_3
			17	133	1 : 1.45 : 0.54	$Al_2(MoO_4)_3$

Note. Data were used from Table 2 and calculation methods according to (33–36). The bold values represent the reference compound giving the best agreement with the experimental results, as discussed in the text. S_{Al}, S_O, and S_{Mo} represent signals originating from aluminium, oxygen, and molybdenum. All areas are normalized to an identical beam current.

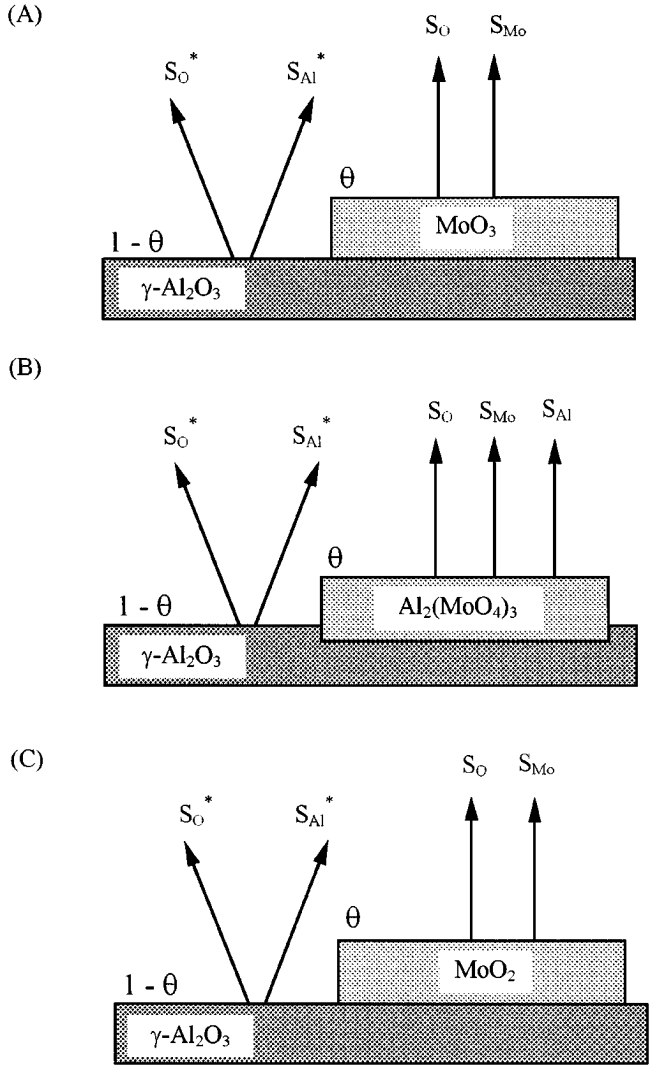

FIG. 12. Schematic representation of the γ-Al_2O_3 surface covered with different molybdenum phases: (A) MoO_3; (B) $Al_2(MoO_4)_3$; and (C) MoO_2 with corresponding LEIS signals (S) of oxygen (O), molybdenum (Mo), and aluminium (Al), where the $*$ designates the signals originating from the support and θ is the percentage of alumina covered.

data for the catalysts are listed in Table 3. The molybdenum and the aluminium ratios and signals were used to calculate the oxygen ratio and total absolute signal for oxygen ($S_O^* + S_O$) (34, 35). When calculating the ratios using $Al_2(MoO_4)_3$ in the model, the aluminium signal originating from this compound (S_{Al}) was corrected for (36). By comparing the experimental signal ratios of the catalysts with the calculated ones using different reference compounds on the γ-Al_2O_3 surface, it can be concluded that for freshly calcined catalysts the molybdenum surface structure is best fitted by $Al_2(MoO_4)_3$. Calculating the absolute oxygen signal ($S_O^* + S_O$) from the measured Al and Mo signals leads to the same conclusion. When the presence of MoO_3 is assumed, the calculated value for oxygen is too high, compared to the measured value (see Table 3).

For hydrogen pretreated catalysts, the differences for the calculated value for oxygen are small, but the best agreement is obtained for the MoO_2 structure.

The amount of coverage of γ-Al_2O_3. Using the absolute areas of the signals, the percentage of the alumina covered with molybdenum species can be calculated. It was already concluded for calcined catalysts that the best agreement was obtained by assuming $Al_2(MoO_4)_3$ on the alumina surface, which yields a coverage of 39% (see Table 2 and (33)), using the molybdenum signals of the catalyst and the reference compound. By subtracting the part of the aluminium signal of the catalyst originating from $Al_2(MoO_4)_3$, assuming $\theta = 39\%$ for the 5 wt% Mo, a value of $S_{Al}^* = 67$ is obtained (37). This corresponds with a fraction of 63% of uncovered alumina, resulting in $\theta = 37\%$ (31). The excellent agreement shows that the method of applying the absolute intensities is reliable and that the porosity of the samples was not an important parameter. The same calculations applied to the calcined 10 wt% Mo catalyst yield a fraction of uncovered γ-Al_2O_3 of 27%, so $\theta = 73\%$ (according to (37) $S_{Al} = 29$), which is also in very good agreement with the value of 77% found by using the Mo intensities. Considering the presence of small amounts of bulk $Al_2(MoO_4)_3$ in the calcined 10 wt% Mo, as was detected by XRD and TEM, it can be concluded that at 10 wt% the maximum adsorption capacity of γ-Al_2O_3 is exceeded to some extent, although only 77% of the alumina is covered. This is in agreement with the observations of van Veen *et al.* (23), where the Mo adsorption levels on γ-Al_2O_3 varied from 8 to 10 wt% Mo, dependent on the pH of the adsorption solution, which is approximately 60 to 70% of the calculated maximum coverage (29).

When freshly pretreated with hydrogen, the fit appeared to be more complicated, resulting in a coverage of γ-Al_2O_3 of 14% (see Table 2 and (33)) or 21% (31), using the Mo signals or the Al signals, respectively, of the catalyst and the reference compounds. The measured oxygen signal is much lower, compared to the calculated value. The XPS analysis suggested that after hydrogen treatment more oxygen is removed from the surface, explaining the lower oxygen signal measured with LEIS. It should be emphasized that the reference compound MoO_2 was not pretreated with hydrogen similarly to the catalyst, but at a lower temperature, this way leaving more lattice oxygen on the surface. From the calculated coverage it is concluded that, when pretreated in hydrogen, approximately 50% less of the alumina is covered with molybdenum than when calcined, so the decrease of the dispersion upon hydrogen pretreatment is estimated at 50%. This suggests that treating a freshly calcined catalyst, containing a monolayer of $Al_2(MoO_4)_3$, with hydrogen results in the formation of a bilayer of MoO_2 on γ-Al_2O_3.

Used catalysts. It is of great interest to know if changes occur in the surface composition due to reaction and

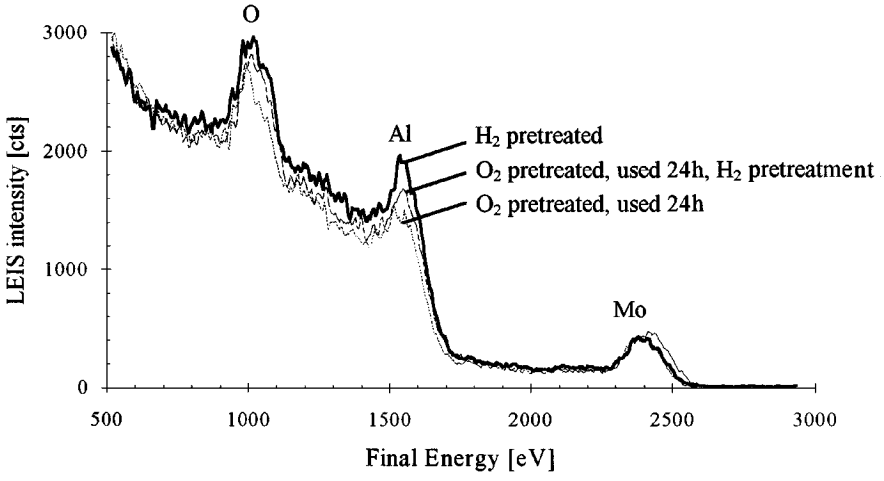

FIG. 13. LEIS spectra of 3 keV $^4He^+$ scattering from various 5 wt% Mo catalysts: hydrogen pretreated fresh, calcined after 24 h on stream at 450°C without treatment and calcined after 24 h on stream at 450°C with a heat treatment in hydrogen prior to the analysis. All spectra were taken after an ion dose of approximately 5×10^{14} ions/cm^2.

whether adsorbed species are present randomly or at specific positions. An attempt was made to elucidate some of these aspects by LEIS analysis on a used catalyst. Figure 13 shows spectra of the 5 wt% Mo catalyst. A fresh hydrogen pretreated catalyst is compared with a calcined one used for 24 h without treatment prior to the measurement and a hydrogen treatment prior to the measurement. Clearly, it can be seen that the molybdenum signal was hardly influenced when submitted to the different conditions. Both the oxygen and the aluminium signal were lower compared to the freshly hydrogen pretreated catalyst, and increased a little when a hydrogen treatment was performed prior to the measurement. This indicates that carbon deposition occurred on the alumina surface and not significantly on the molybdenum. Also, the fact that the spectra are similar when hydrogen pretreated or calcined and used for 24 h indicates that a similar molybdenum surface structure is formed under these conditions.

CONCLUSIONS

Previous work reported the existence of two mechanisms for the formation of acetonitrile on γ-Al_2O_3-supported molybdenum catalysts (6). When freshly calcined, acetonitrile is formed via an ammoxidation mechanism where the lattice oxygen of the catalyst is consumed by forming water. Steady-state catalysts formed acetonitrile via an oxidative ammonolysis mechanism, without the consumption of lattice oxygen, indicating that the catalyst had reached chemical and structural equilibrium. Both mechanisms can be active separately and simultaneously, depending on the catalyst pretreatment and time on stream. The aim of this study was to elucidate the relationship between catalytic activity and solid state properties of the catalyst.

All fresh catalysts were very homogeneous and no small molybdenum-containing particles were visible on the alumina surface, indicating that the active phase was highly dispersed. It was concluded that when the maximum adsorption capacity of the alumina, estimated at 8–9 wt% Mo, is exceeded, the excess molybdenum is used to form bulk structures separately from the highly dispersed Mo/γ-Al_2O_3. When calcined, these bulk structures consisted of $Al_2(MoO_4)_3$ and appeared at 10 and 15 wt% Mo. When pretreated with hydrogen, the bulk structure consisted of MoO_2 and was formed at 15 wt% Mo.

An attempt was made to identify the highly dispersed phase and to estimate quantitatively the coverage of the support with the active material. By applying a model of different reference compounds, it was concluded that 39 and 79% (±3%), respectively, of the γ-Al_2O_3 of a freshly calcined catalyst, with 5 and 10 wt% Mo, is covered with $Al_2(MoO_4)_3$. This indicated that adsorption occurs at specific sites and that approximately one quarter of the γ-Al_2O_3 surface is not capable of accommodating molybdenum.

On fresh catalysts pretreated with hydrogen, it was observed that the reducibility increases with increasing Mo content due to the presence of polymeric molybdate species which are easier to reduce. Pretreatment with hydrogen induced a MoO_2-like surface which contained more Mo(IV) species and less lattice oxygen on the surface. A decrease in dispersion of approximately 50% was observed upon hydrogen pretreatment compared to calcination.

It was concluded that Mo(VI) sites are active in the ammoxidation mechanism on calcined catalysts in the semi-steady state and exist in a highly dispersed $Al_2(MoO_4)_3$ phase, containing tetrahedrally coordinated molybdenum. It was suggested that the large crystals, present at high

Mo content, were responsible for the steep profile for acetonitrile formation (see Fig. 1, solid line), due to the large amount of removable lattice oxygen present in these bulk structures.

When pretreated with hydrogen, lattice oxygen is still removed under reaction conditions, indicating that the ammoxidation and oxidative ammonolysis mechanisms can be active simultaneously. by removing part of the lattice oxygen through hydrogen pretreatment, a gradual profile reaching steady state can be obtained for all Mo coverages tested (see Fig. 1, dotted line).

At steady state, the catalyst has reached structural and chemical equilibrium, independent of the pretreatment applied. Acetonitrile is formed solely via oxidative ammonolysis in this period. This stable molybdenum structure was identified as MoO_2, containing both Mo(IV) and Mo(VI) ions. For catalysts at steady state a decrease in dispersion was estimated also at approximately 50%, although the steady-state catalysts were more active than their calcined analogues at semi-steady-state. This suggests that following hydrogen treatment, the monolayer of $Al_2(MoO_4)_3$ present on calcined catalysts is converted to a bilayer of MoO_2. No chemical interaction occurs between the support and the active phase, as was the case for $Al_2(MoO_4)_3$ present on calcined catalysts. Thus, we conclude that a decrease in interaction between the support and the molybdenum phase induces higher catalytic activity.

Under reaction conditions, some carbon deposition was observed which preferentially occurred on the alumina surface, explaining the absence of catalyst deactivation caused by carbon poisoning.

ACKNOWLEDGMENTS

We thank A. M. Elemans-Meyring for collecting the X-ray diffraction data and R. P. J. M. Houben for the catalyst preparation and testing. Financial support of this research work by the Dutch Organization for Scientific Research (NWO/SON) is gratefully acknowledged.

REFERENCES

1. Grasselli, R. K., and Burrington, J. D., *Adv. Catal.* **30**, 133 (1981).
2. Burrington, J. D., Kartisek, C. T., and Grasselli, R. K., *J. Catal.* **87**, 363 (1984).
3. Allison, J. N., and Goddard, W. A., *in* "Solid State Chemistry in Catalysis," Vol. 23. Am. Chem. Soc., Washington, DC, 1985.
4. Andrushkevich, T. V., *Catal. Rev.-Sci. Eng.* **35**, 213 (1993).
5. Dadyburjur, D. B., Jewur, S. S., and Ruckenstein, E., *Rev.-Sci. Eng.* **19**, 293 (1979).
6. Peeters, I., van Grondelle, J., and Van Santen, R. A., *in* "Heterogeneous Hydrocarbon Oxidation" (B. K. Warren and S. T. Oyama, Eds.), Vol. 638, p. 319. Am. Chem. Soc., Washington, DC, 1996. [ACS Symposium Series]
7. Rajagopal, S., Marini, H. J., Marzari, J. A., and Miranda, R., *J. Catal.* **147**, 417 (1994).
8. Defossé, C., Canesson, P., Rouxhet, P. G., and Delmon, B., *J. Catal.* **51**, 269 (1978).
9. Shalvoy, R. B., and Reucroft, P. J., *J. Electron Spectrosc. Relat. Phenom.* **12**, 351 (1977).
10. Angevine, P. J., Vartuli, J. C., and Delgass, W. N., *in* "Proc. 6th Int. Concr. Catal. 1976," Vol. 2, p. 611.
11. Kerkhof, F. P. J. M., and Moulijn, J. A., *J. Phys. Chem.* **83**(12), 1612 (1979).
12. Kuipers, H. P. C. E., Van Leuven, H. C. E., and Visser, W. M., *Surf. Interface Anal.* **8**, 235 (1986).
13. Brongersma, H. H., Groenen, P. A. C., and Jacobs, J.-P, *in* "Science of Ceramic Interfaces II" (J. Nowotny, Ed.), p. 113. Elsevier, Amsterdam, 1994.
14. Peeters, I., Ph.D. thesis, Eindhoven University of Technology, The Netherlands, 1996.
15. Mulcahy, F. M., Houalla, M., and Hercules, D. M., *Anal. Chem.* **62**, 2232 (1990).
16. Eberhardt, M. A., Houalla, M., and Hercules, D. M., *Surf. Interface Anal.* **20**, 766 (1993).
17. Fiedor, J. N., Houalla, M., Proctor, A., and Hercules, D. M., *Surf. Interface Anal.* **23**, 234 (1995).
18. JCPDS-card 23-764.
19. JCPDS-card 32-671.
20. Giordano, N., Bart, J. C. J., Vaghi, A., Castellan, A., and Martinotti, G., *J. Catal.* **36**, 81 (1975).
21. Sonnemans, J., and Mars, P., *J. Catal.* **31**, 209 (1973).
22. Asmolov, G. N., and Krylov, O. V., *Kinet. Katal.* **11**, 1028 (1970).
23. Van Veen, J. A. R., Hendriks, P. A. J. M., Romers, E. J. G. M., and Andréa, R. R., *J. Phys. Chem.* **94**, 5275 (1990).
24. Scofield, J. H., *J. Electr. Spectr. Rel. Phenom.* **8**, 129 (1976).
25. Seah, M. P., and Dench, W. A., *Surf. Interface Anal.* **1**(1), 1 (1979).
26. Grünert, W., Stakheev, A. Yu, Mörke, W., Feldhaus, R., Anders, K., Shpiro, E. S., and Minachev, Kh. M., *J. Catal.* **135**, 269 (1992).
27. Haber, J., Marczewski, W., Stoch, J., and Ungier, L., *Ber. Bunsen-Ges.* **79**, 970 (1975).
28. De Jong, A. M., Borg, H. J., Van IJzendoorn, L. J., Soudant, V. G., Figure, M., De Beer, V. H. J., Van Veen, J. A. R., and Niemantsverdriet, J. W., *J. Phys. Chem.* **97**, 6477 (1993).
29. 100 g catalyst contains 5 g Mo = 0.0521 mol = 3.119×10^{22} Mo clusters = 6.3×10^3 m^2 (* 20 Å^2); 95 g γ-Al_2O_3 = 19×10^3 m^2 (200 m^2/g); $\theta = 6.277/19 * 100\% = 33\%$; the theoretical maximum coverage: 1 g γ-Al_2O_3 = 200 m^2 can support 10^{21} Mo clusters = 1.7×10^{-3} mol = 0.16 g = 14 wt%.
30. Sonnemans, J., and Mars, P., *J. Catal.* **31**, 209 (1973).
31. Percentage of free γ-$Al_2O_3 = 1 - \theta = S_{Al}$ (Table 3; 5 wt% Mo calcined measured)/S_{Al} (Table 2; γ-Al_2O_3) = 75/106 * 100% = 71%; so $\theta = 29\%$.
32. Brongersma, H. H., and Van Leerdam, G. C., *in* "Fundamental Aspects of Heterogeneous Catalysis Studied by Particle Beams" (H. H. Brongersma and R. A. van Santen, Eds.), p. 283. Plenum, New York, 1991.
33. $\theta = S_{Mo}$ (Table 3; measured)/S_{Mo} (Table 2; molybdenum reference compound) * 100%.
34. Calculation Table 3: $S_O + S_O^* = \theta * S_O$ (Table 2; Mo compound) + $(1 - \theta) * S_O$ (Table 2; γ-Al_2O_3).
35. Example oxygen ratio calculation for the calcined 5 wt% Mo catalyst with data from Table 2: 1 Al accounts for 1.10 O; 1.41 Mo (Table 3) accounts for 0.78 (Table 2 reference MoO_3) * 1.41 = 1.10 O; total of O: 1.10 + 1.10 = 2.20 (see Table 3).
36. Example oxygen ratio (r_O) calculation for the calcined 5 wt% Mo catalyst with correction for $Al_2(MoO_4)_3$ with data from Table 2: $\theta = 0.39$: Table 2: $r_O = (1 - \theta) * r_O(\gamma\text{-}Al_2O_3) + \theta * r_O(Al_2(MoO_4)_3) = 0.61 * 1.10 + 0.39 * 9.65 = 4.43$ (see Table 3).
37. Correction measured S_{Al} for the contribution of $Al_2(MoO_4)_3$: S_{Al} (γ-Al_2O_3) = S_{Al} (measured) $- \theta * S_{Al}(Al_2(MoO_4) = 75 - 0.39 * 20 = 67$.